

Frontal face authentication using morphological elastic graph matching

C. Kotropoulos A. Tefas I. Pitas

Department of Informatics, Aristotle University of Thessaloniki

Box 451, Thessaloniki 540 06, GREECE

E-mail :`{costas,tefas,pitas}@zeus.csd.auth.gr`

This work was carried out within the framework of European Union ACTS research project (AC-102) “Multi-modal Verification Techniques for Tele-services and Security Applications” (M2VTS).

Abstract

A novel dynamic link architecture based on multiscale morphological dilation-erosion is proposed for frontal face authentication. Instead of a set of Gabor filters tuned to different orientations and scales, multiscale morphological operations are employed to yield a feature vector at each node of the reference grid. Linear projection algorithms for feature selection and automatic weighting of the nodes according to their discriminatory power succeed to increase the authentication capability of the method. The performance of morphological dynamic link architecture is evaluated in terms of the receiver operating characteristic in the M2VTS face image database. The comparison with other frontal face authentication algorithms indicates that the morphological dynamic link architecture with discriminatory power coefficients is the best algorithm with respect to the equal error rate achieved.

I. INTRODUCTION

Automated face recognition has exhibited a tremendous growth for more than two decades [1]. An approach that exploits both the grey-level information and the geometrical one is the so-called *Dynamic Link Architecture* (DLA) [2]-[5]. The algorithm is split in the training and recall phase. In the training phase, a sparse grid for each person included in the reference set is built. The grid is overlaid on the facial region of a person's digital image and the response of a set of 2D Gabor filters tuned to different orientations and scales is measured at the grid nodes. In the recall phase, the reference grid of a claimed person is overlaid on the face image of a test person and is deformed so that a cost function is minimized.

A novel dynamic link architecture based on multiscale morphological dilation-erosion, the so called *morphological dynamic link architecture* (MDLA), is proposed for frontal face authentication. The multiscale dilation-erosion of the image by a scaled structuring function [6] is employed to yield a feature vector at each grid node instead of a set of Gabor filters tuned to different orientations and scales. In the test phase, multiscale morphological operations are applied over the entire image of a candidate before dynamic link matching. Thus, the computation of the time consuming Gabor-based feature vectors that rely on floating point arithmetic operations (i.e., FFTs or convolutions) is avoided. Moreover, no filter design is needed. Additional reasons which support this decision are: (1) Scale-space morphological techniques are able to find the true size of the object in an image smoothed to a particular size. (2) The scale parameter has a straightforward interpretation since it is associated with the area of the domain of the structuring function. (3) Dilations and erosions can be computed very fast either by running min/max

algorithms [9] or by recursive separable computations or by scale recursive computations (see discussion in Section II). (4) Dilations and erosions deal with the local extrema in an image. Therefore, they are well-suited for facial feature representation, because key facial features are associated either to local minima (e.g. eyebrows/eyes, nostrils, mouth corners etc.) or to local maxima (e.g. the nose tip). In the paper, the details of feature extraction/selection and feature matching are discussed. The performance of the proposed morphological dynamic link architecture (MDLA) is evaluated in terms of the receiver operating characteristic (ROC) for several threshold selections on the matching error in the database of the European Union project “Multimodal Verification Techniques for Teleservices and Security Applications” (abbreviated as M2VTS database) [10].

The outline of the paper is as follows. Section II describes the morphological dynamic link architecture. Experimental results are shown in Section III and conclusions are drawn in Section IV.

II. MORPHOLOGICAL DYNAMIC LINK ARCHITECTURE

An alternative to linear techniques used for generating an information pyramid is the scale-space morphological techniques. In this paper, we propose the substitution of Gabor-based feature vectors used in dynamic link matching by the *multiscale morphological dilation-erosion* [6]. Let \mathcal{R} and \mathcal{Z} denote the set of real and integer numbers, respectively. Given an image $f(\mathbf{x}) : \mathcal{D} \subseteq \mathcal{Z}^2 \rightarrow \mathcal{R}$ and a structuring function $g(\mathbf{x}) : \mathcal{G} \subseteq \mathcal{Z}^2 \rightarrow \mathcal{R}$, the dilation of the image $f(\mathbf{x})$ by $g(\mathbf{x})$ is denoted by $(f \oplus g)(\mathbf{x})$. Its complementary operation, the erosion, is denoted by $(f \ominus g)(\mathbf{x})$ [9]. The multiscale dilation-erosion of the image $f(\mathbf{x})$ by $g_\sigma(\mathbf{x})$ is defined by [6]:

$$(f \star g_\sigma)(\mathbf{x}) = \begin{cases} (f \oplus g_\sigma)(\mathbf{x}) & \text{if } \sigma > 0 \\ f(\mathbf{x}) & \text{if } \sigma = 0 \\ (f \ominus g_{|\sigma|})(\mathbf{x}) & \text{if } \sigma < 0 \end{cases} \quad (1)$$

where σ denotes the scale parameter of the structuring function. Several structuring functions can be chosen [6]. It has been found that the choice of the structuring function affects the verification capability of the proposed technique to a margin of $\pm 0.5\%$ in terms of the equal error rate, but it does affect the time required to compute the dilations and erosions. For a flat structuring function, we may apply either running max/min calculations [9] or scale-recursive

ones. The latter computations are based on the observation:

$$(f \oplus g_{\sigma+1})(x_1, x_2) = \max\{(f \oplus g_{\sigma})(x_1, x_2), \max_{(z_1, z_2) \in \Delta G(\sigma+1)} \{f(x_1 + z_1, x_2 + z_2)\}, \max\{f(x_1 \pm (\sigma + 1), x_2 \pm (\sigma + 1))\}\} \quad (2)$$

where $\Delta G(\sigma + 1) = \{(z_1, z_2) \in \mathcal{Z}^2 : (z_1^2 + z_2^2) > \sigma^2, (z_1^2 + z_2^2) \leq (\sigma + 1)^2, |z_1| \leq \sigma, |z_2| \leq \sigma\}$. The set $\Delta G(\sigma + 1)$ possesses a symmetry and can easily be determined prior to the computation of dilations. A similar recursive computation can be applied for minima as well. The outputs of multiscale dilation-erosion for $\sigma = -\sigma_m, \dots, \sigma_m$ form the feature vector located at the grid node \mathbf{x} :

$$\mathbf{j}(\mathbf{x}) = ((f \star g_{\sigma_m})(\mathbf{x}), \dots, (f \star g_1)(\mathbf{x}), f(\mathbf{x}), (f \star g_{-1})(\mathbf{x}), \dots, (f \star g_{-\sigma_m})(\mathbf{x})). \quad (3)$$

The parameter σ_m is upper bounded by the half of the minimal distance between two nodes of the sparse grid that is to be created. The value $\sigma_m = 9$ has been used in all experiments reported in this paper. An 8×8 sparse grid has been created by measuring the feature vectors $\mathbf{j}(\mathbf{x})$ at equally spaced nodes over the output of the face detection algorithm [8], a variant of the method proposed by Yang and Huang [7]. Fig. 1 depicts the output of multiscale dilation-erosion for the various scales used. The first nine pictures starting from the upper left picture are dilated images and the remaining nine are eroded images. It is seen that multiscale dilation-erosion captures important information for key facial features such as the eyebrows, eyes, nose tip, nostrils, lips, face contour, etc.

Frequently, linear projection algorithms are used to reduce the dimensionality of the feature vectors. Two are the most popular linear projection algorithms: the *Karhunen-Loeve or Principal Component Analysis* (PCA) that does not employ category information and the *linear discriminant analysis* (LDA) that exploits the category labels. Representations based on PCA are useful to image reconstruction/ compression tasks [12]. Let $\mathbf{j}'(\mathbf{x}_l) = \mathbf{j}(\mathbf{x}_l) - \mathbf{m}(\mathbf{x}_l)$ be the normalized feature vector at node \mathbf{x}_l , where $\mathbf{j}(\mathbf{x}_l) = (j_1(\mathbf{x}_l), \dots, j_{2\sigma_m+1}(\mathbf{x}_l))^T$, and $\mathbf{m}(\mathbf{x}_l)$ be the mean feature vector. The eigenvectors $\mathbf{e}_i(\mathbf{x}_l)$ that correspond to the p largest eigenvalues of the covariance matrix of feature vectors $\mathbf{j}'(\mathbf{x}_l)$ are computed and the PCA projected feature vector is given by:

$$\tilde{\mathbf{j}}(\mathbf{x}_l) = \begin{bmatrix} \mathbf{e}_1^T(\mathbf{x}_l) \\ \vdots \\ \mathbf{e}_p^T(\mathbf{x}_l) \end{bmatrix} \quad \mathbf{j}'(\mathbf{x}_l) = \mathbf{P}(\mathbf{x}_l) \mathbf{j}'(\mathbf{x}_l) \quad (4)$$

where T denotes the transposition operator. The resulting vector $\tilde{\mathbf{j}}(\mathbf{x}_l)$ is comprised by the so-called *most expressive features* [13]. It is of dimensions $p \times 1$ with $p \leq (2\sigma_m + 1)$.

It is well known that there is no guarantee that the most expressive features alone are necessarily good candidates for discriminating among classes defined by a set of samples [12], [13]. Such an optimality can be achieved by employing Linear Discriminant Analysis (LDA). The feature vectors produced after the LDA projection are called *most discriminating features* (MDFs) [13]. In this paper, the LDA is applied after having reduced the dimensionality of raw feature vectors by PCA. This is a method that allows us to cope with the so-called *curse of dimensionality* outlined in Section III. A similar procedure has been used in Fisherfaces [14]. We are interested in applying the LDA locally at each grid node. Let \mathcal{S} be the entire set of feature vectors at a grid node and \mathcal{S}_k be the subset of features vectors at this node extracted from the frontal face images of the k -th person in the database. The local LDA scheme determines a weighting matrix ($d \times p$), \mathbf{V}_k , such that the ratio:

$$\mathcal{M}_k = \frac{\text{tr} \left[\mathbf{V}_k \left\{ \sum_{\tilde{\mathbf{j}} \in \mathcal{S}_k} (\tilde{\mathbf{j}} - \tilde{\mathbf{m}}_k)(\tilde{\mathbf{j}} - \tilde{\mathbf{m}}_k)^T \right\} \mathbf{V}_k^T \right]}{\text{tr} \left[\mathbf{V}_k \left\{ \sum_{\tilde{\mathbf{j}} \in (\mathcal{S} - \mathcal{S}_k)} (\tilde{\mathbf{j}} - \tilde{\mathbf{m}}_k)(\tilde{\mathbf{j}} - \tilde{\mathbf{m}}_k)^T \right\} \mathbf{V}_k^T \right]} = \frac{\text{tr} [\mathbf{V}_k \mathbf{W}_k \mathbf{V}_k^T]}{\text{tr} [\mathbf{V}_k \mathbf{B}_k \mathbf{V}_k^T]} \quad (5)$$

is minimized, where $\tilde{\mathbf{m}}_k$ is the class-dependent mean vector of the most expressive feature vectors. In (5) the explicit dependence on \mathbf{x} is omitted for notation simplicity. The solution of the generalized eigenvalue problem (5), i.e., the row vectors of \mathbf{V}_k (\mathbf{v}_{ik} , $i = 1, \dots, d$), is given by the eigenvectors that correspond to the d largest in magnitude eigenvalues of $\mathbf{W}_k^{-1} \mathbf{B}_k$ provided that both \mathbf{W}_k and \mathbf{B}_k are invertible. The stable computation procedure proposed in [13] has been used for the minimization of (5).

We shall confine ourselves to $d = 2$ for facilitating the discussion. Let the superscripts t and r denote a test and a reference person (or grid), respectively. Having found the weighting matrix $\mathbf{V}_k(\mathbf{x}_l)$, for the l -th node of the k -th person, we project the most expressive feature vector at this node onto the plane defined by $\mathbf{v}_{1k}(\mathbf{x}_l)$ and $\mathbf{v}_{2k}(\mathbf{x}_l)$, i.e., $\check{\mathbf{j}}(\mathbf{x}_l^r) = \mathbf{V}_k [\mathbf{P}(\mathbf{x}_l) (\mathbf{j}(\mathbf{x}_l^r) - \mathbf{m}_l) - \tilde{\mathbf{m}}_{kl}]$. Let us suppose that a test person claims the identity of the k -th person. The test most discriminating feature vector at the l -th node can be found then similarly. The quality of the match between a test and a reference feature vector is evaluated by taking into account both the L_2 norm of their difference and by penalizing the grid deformations, as in DLA [2]. Lades et al. argue that a two stage coarse-to-fine optimization procedure suffices for the minimization of such a cost function [2]. The above mentioned approach is proven inadequate in our experiments.

Accordingly, we propose: (i) to exploit the face detection outcome provided by the hierarchical rule-based system [8] for initializing the minimization of the cost function, and (ii) to replace the two stage optimization procedure by a probabilistic hill climbing algorithm (i.e., a simulated annealing algorithm) that is reminiscent of the Algorithm 1.4 [11, p. 12] that does not make distinction between coarse and fine matching. Figure 2 depicts the grids formed in the matching procedure of a test person with himself and with another person for a pair of test persons extracted from the M2VTS database.

An alternative scheme aiming at weighting the grid nodes in elastic graph matching by a coefficient that depends on the first and second-order statistics of the matching errors is proposed as well. Let $C_v(\mathbf{j}(\mathbf{x}_l^t), \mathbf{j}(\mathbf{x}_l^r))$ denote the signal similarity measure at node l . The signal similarity measure at node l can be weighted by using class-dependent coefficients $DP_l(\mathcal{S}_r)$, the so-called *discriminatory power coefficients*, so that when person t claims the identity of person r the distance between them is computed by:

$$D(t, r) = \sum_{l \in \mathcal{V}} \frac{DP_l(\mathcal{S}_r) C_v(\mathbf{j}(\mathbf{x}_l^t), \mathbf{j}(\mathbf{x}_l^r))}{\sum_{i \in \mathcal{V}} DP_i(\mathcal{S}_r)} \quad (6)$$

where \mathcal{S}_r denotes the class of the reference person r . A plausible measure of the discriminatory power of the grid node l for the class \mathcal{S}_r is the *Fisher's Linear Discriminant* function that takes into consideration both the difference between the mean intra-/inter- matching errors and the compactness of the clusters of intra-/inter- class matching errors. It yields a discriminatory power coefficient for the grid node l of the reference person having the form:

$$DP_l(\mathcal{S}_r) = \frac{(m_{\text{inter}}(\mathcal{S}_r, l) - m_{\text{intra}}(\mathcal{S}_r, l))^2}{\text{var}_{\text{inter}}(\mathcal{S}_r, l) + \text{var}_{\text{intra}}(\mathcal{S}_r, l)} \quad (7)$$

where $m_{\text{inter}}(\mathcal{S}_r, l)$ is the mean intra-class matching error for the class \mathcal{S}_r , $m_{\text{intra}}(\mathcal{S}_r, l)$ is the mean inter-class matching error between the class \mathcal{S}_r and the class $(\mathcal{S} - \mathcal{S}_r)$ and $\text{var}_{\text{inter}}(\mathcal{S}_r, l)$, $\text{var}_{\text{intra}}(\mathcal{S}_r, l)$ are the corresponding variances at grid node l . The discriminatory power coefficients (7) can easily be computed during the application of the verification algorithm to any database following any experimental protocol. They can easily be modified when persons are added to or deleted from the database, because the computation of the mean matching errors and the variances of matching errors can be made incrementally. This is not the case with linear projections when they are applied to *select the most discriminating features*, because so far only the asymptotic convergence of recursively computed eigenvectors to the true ones has been theoretically established. In our case, we have a limited number of feature vectors available.

III. EXPERIMENTAL RESULTS

The Morphological Dynamic Link Architecture has been tested on the M2VTS database [10]. The database contains 37 persons' video data, which include speech consisting of uttering digits and image sequences of rotated heads. Four recordings (i.e., shots) of the 37 persons have been collected. The luminance information at a resolution of 286×350 pixels has been considered only in our experiments. Four experimental sessions have been implemented by employing a "leave one out" principle. The experimental protocol is pictorially described in Figure 3, where BP , BS , CC , ..., XM are the identity codes of the persons included in the database. The training set is built of 3 (out of 4) shots of 36 (out of 37) persons. The objective in the training procedure is to determine a threshold on the distance measures. Let $D_{(l)}(BS; 4, BP)$ denote the l -th order statistic in the set of impostor distances for BS , when person BP from shot 4 is excluded. A threshold can be chosen as $T_{BS}(4, BP) = D_{(1+Q)}(BS; BP, 4)$ where $Q = 0, 1, 2, \dots$. In the test procedure, three shots create the training set, while the fourth one is used as the test set. Each person is considered as an impostor in turn, while the remaining 36 persons are used as clients. Each client tries to access under its own identity, while the impostor tries to access pretending the identity of each client. The reference grids derived for each client during the training procedure are matched and adapted to the feature vectors computed at every pixel of a test face image using MDLA. The resulting distance measure is compared then against the threshold having been determined in the training procedure. The minimum intra-class/inter-class distance is used in the comparisons, i.e., $D(BP_4, \{BS\}) = \min_{j=1}^3 \{D(BP_4, BS_j)\}$, where the first ordinate in distance computations denotes the face image of a test person and the second ordinate denotes a reference grid for a client. For a particular choice of parameter Q , a collection of thresholds is determined that defines an *operating state*. For each operating state, a false acceptance rate (FAR) and a false rejection rate (FRR) can be computed. By varying the parameter Q , several operating states result. Accordingly, we may create a plot of FRR versus FAR with the operating state being an implicit set of parameters. This plot is the *Receiver Operating Characteristic* (ROC) curve of the verification technique. The ROC curve of MDLA when a scaled hemisphere is used as a structuring function is plotted in Figure 4. The Equal Error Rate of MDLA (i.e., the operating state having FAR equal to FRR) is 9.35%.

To enhance the verification capability of the proposed method, linear projection algorithms are employed for feature selection. The practical reason for employing PCA is the following: Let \mathcal{J}

and N denote the dimensionality of the feature vector (i.e., $\mathcal{J} = 19$ for raw feature vectors) and the number of feature vectors available at each grid node. LDA breaks down if the inequalities $N \geq \mathcal{J} + 2$ and $\mathcal{J} \geq 2$ are not satisfied. To cope with the curse of dimensionality, we have either to extract additional frontal images for each person or to augment the original frontal images with others produced by adding slightly Gaussian noise to them, as is proposed in [12]. However, for clients the problem remains unsolved, because N varies between 10 and 42. The number of feature vectors for impostors is quite large (i.e., N is between 793 and 1012) and does not pose any difficulty. Accordingly, to anticipate the lack of feature vectors for clients we apply first the principal component analysis for raw feature vector dimensionality reduction and the discriminant analysis afterwards. It has been found that six principal components can approximate the feature vectors with a mean squared error less than 5%. Two cases are considered then, i.e., the derivation of one and two most discriminating features. The ROC curves of the enhanced MDLA are plotted in Figure 4. The best EER ($\approx 5.4\%$) is obtained when two most discriminating features are used at each grid node. Further improvements are obtained when the node weighting procedure is applied to the raw MDLA. The ROC of the MDLA with node weighting coefficients given by (7) is plotted in Figure 4 as well. It is seen that the EER of MDLA with node weighting coefficients is approximately 3.7%. The ensemble $\{\text{test images, verification algorithm}\}$ is a source of binary events: 1 for false rejection (or false acceptance) and 0 for no error with probability p_{FR} (or p_{FA}) of drawing a 1 and $(1 - p_{FR})$ - or $(1 - p_{FA})$, respectively - of drawing a 0. These events can be described by Bernoulli trials. Let us denote by \hat{p}_{FR} and \hat{p}_{FA} the estimates of FRR and FAR, respectively. The exact γ confidence interval of p_{FR} and p_{FA} is the segment between the two roots of the quadratic equation [17]:

$$(p - \hat{p})^2 = \frac{z_{(1+\gamma)/2}^2}{N} p (1 - p), \quad p = p_{FR}, p_{FA}, \quad N = 5328 \quad (8)$$

where z_u is the u -percentile of the standard Gaussian distribution having zero mean and unit variance. The $\gamma = 95\%$ confidence interval of FAR and FRR is indicated with a horizontal and a vertical error bar, respectively, for all ROCs in Figure 4.

We conclude the section by comparing the EER achieved by the proposed methods with the best EERs achieved by other frontal face authentication algorithms developed within M2VTS project. The EERs and the corresponding citations are tabulated in Table I. From the inspection of the table, it is seen that the MDLA with discriminatory power coefficients is ranked as the

first method with respect to EER.

IV. CONCLUSIONS

A novel dynamic link architecture based on multiscale morphological dilation-erosion has been proposed for frontal face authentication. Linear projection algorithms have been used for feature selection. Furthermore, an automatic weighting of the nodes according to their discriminatory power based on their matching errors has been proposed. The performance of the proposed morphological dynamic link architecture has been tested in terms of the receiver operating characteristic for several threshold selections on the matching error in the M2VTS database.

REFERENCES

- [1] R. Chellapa, C.L. Wilson, and S. Sirohey, "Human and machine recognition of faces: A survey," *Proceedings of the IEEE*, vol. 83, no. 5, pp. 705-740, May 1995.
- [2] M. Lades, J.C. Vorbrüggen, J. Buhmann, J. Lange, C. v.d. Malsburg, R.P. Würtz, and W. Konen, "Distortion invariant object recognition in the Dynamic Link Architecture," *IEEE Trans. on Computers*, vol. 42, no. 3, pp. 300-311, March 1993.
- [3] L. Wiskott, J.-M. Fellous, N. Krüger, and C. v.d. Malsburg, "Face recognition by elastic bunch graph matching," *IEEE Trans. on Pattern Analysis and Machine Intelligence*, vol. 19, no. 7, pp. 775-779, July 1997.
- [4] B. Duc, S. Fischer, and J. Bigün, "Face authentication with Gabor information on deformable graphs," *IEEE Trans. on Image Processing*, to appear.
- [5] N. Krüger, "An algorithm for the learning of weights in discrimination functions using a priori constraints," *IEEE Trans. on Pattern Analysis and Machine Intelligence*, vol. 19, no. 7, pp. 764-768, July 1997.
- [6] P.T. Jackway, and M. Deriche, "Scale-space properties of the multiscale morphological dilation-erosion," *IEEE Trans. on Pattern Analysis and Machine Intelligence*, vol. 18, no. 1, pp. 38-51, January 1996.
- [7] G. Yang, and T.S. Huang, "Human face detection in a complex background," *Pattern Recognition*, vol. 27, no. 1, pp. 53-63, 1994.
- [8] C. Kotropoulos, and I. Pitas, "Rule-based face detection in frontal views," in *Proc. of the IEEE Int. Conf. on Acoust, Speech and Signal Proc.(ICASSP 97)*, pp. 2537-2540, Munich, Germany 1997.
- [9] I. Pitas, and A.N. Venetsanopoulos, *Nonlinear Digital Filters: Principles and Applications*. Norwell, MA: Kluwer Academic Publ., 1990.
- [10] S. Pigeon, and L. Vandendorpe, "The M2VTS multimodal face database," in *Lecture Notes in Computer Science: Audio- and Video- based Biometric Person Authentication* (J. Bigün, G. Chollet and G. Borgefors, Eds.), vol. 1206, pp. 403-409, 1997.
- [11] R.H.J.M. Otten, and L.P.P.P. van Ginneken, *The Annealing Algorithm*. Norwell, MA: Kluwer Academic Publ., 1989.
- [12] K. Etemad, and R. Chellappa, "Discriminant Analysis for Recognition of Human Face Images," in *Lecture*

- Notes in Computer Science: Audio- and Video- based Biometric Person Authentication* (J. Bigün et al., Eds.), vol. 1206, pp. 127–142, 1997.
- [13] D.L. Swets, and J. Weng, “Using discriminant eigenfeatures for image retrieval,” *IEEE Trans. on Pattern Analysis and Machine Intelligence* vol. 18, no. 8, pp. 831–837, August 1996.
- [14] P.N. Belhumeur, J.P. Hespanha, and D.J. Kriegman, “Eigenfaces vs. Fisherfaces: Recognition using class specific linear projection,” *IEEE Trans. on Pattern Analysis and Machine Intelligence* vol. 19, no. 7, pp. 711–720, July 1997.
- [15] J. Matas, K. Jonsson, and J. Kittler, “Fast face localisation and verification,” in *Proc. of British Machine Vision Conference*, 1997.
- [16] S. Pigeon, and L. Vandendorpe, “Image-based multimodal face authentication,” *Signal Processing*, vol. 69, pp. 59–79, August 1998.
- [17] A. Papoulis, *Probability, Random Variables and Stochastic Processes*, 3/e. N.Y.:McGraw-Hill, 1991.

TABLE I

BEST EERs ACHIEVED BY FRONTAL FACE AUTHENTICATION ALGORITHMS WITHIN M2VTS PROJECT.

Method	EER (%)
morphological dynamic link architecture with discriminatory power coefficients	3.7
Optimized robust correlation [15]	4.8
Elastic graph matching based on Gabor wavelets with local discriminants [4]	5.4
Grey level frontal face matching [16]	8.5



Fig. 1. Dilated and eroded images with a scaled hemisphere for scales 1–9.

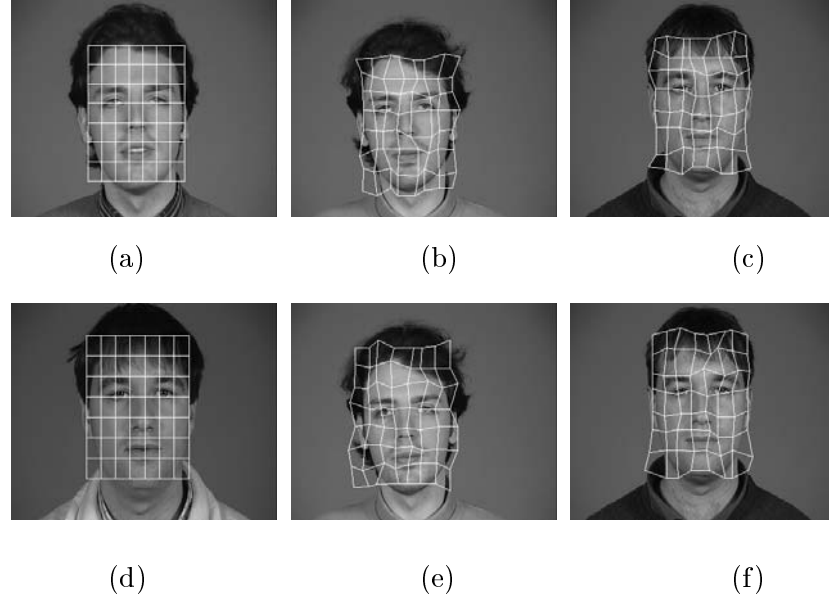


Fig. 2. Grid matching procedure in MDLA: (a) Model grid for person *BP*. (b) Best grid for test person *BP* after elastic graph matching with the model grid. (c) Best grid for test person *BS* after elastic graph matching with the model grid for person *BP*. (d) Model grid for person *BS*. (e) Best grid for test person *BP* after elastic graph matching with the model grid for *BS*. (f) Best grid for test person *BS* after elastic graph matching with the model grid.

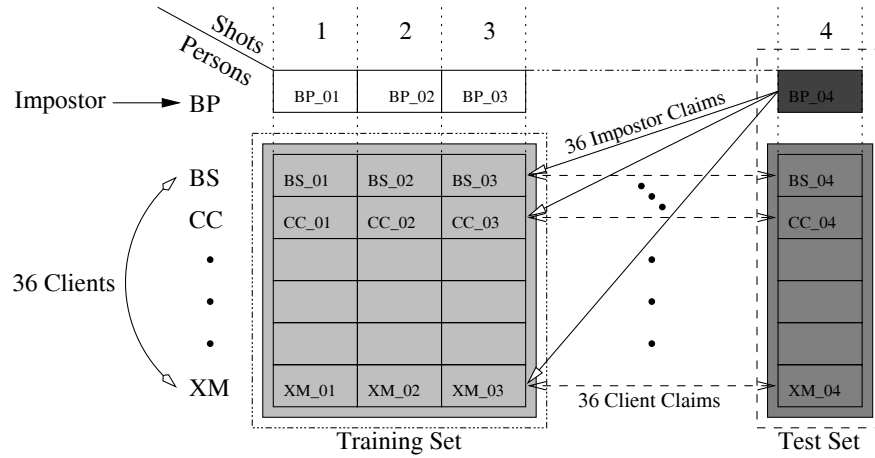


Fig. 3. Experimental Protocol.

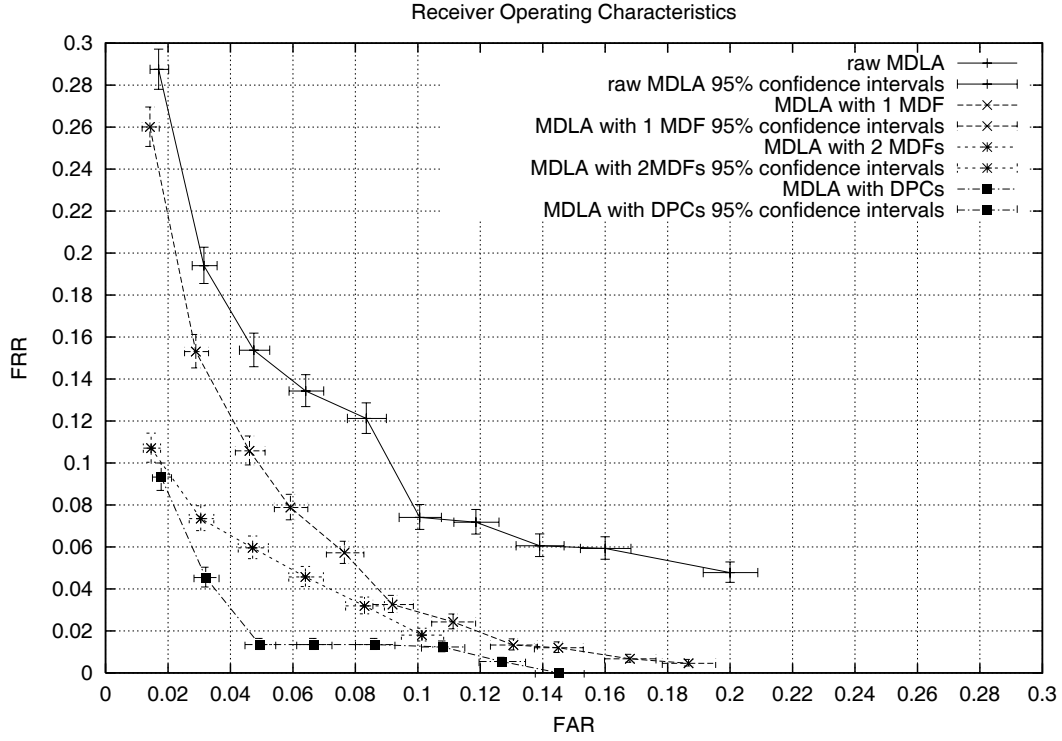


Fig. 4. Receiver Operating Characteristics of MDLA with and without most discriminating features as well as when discriminatory power coefficients are derived at each grid node. The 95% confidence interval of FAR and FRR is indicated with horizontal and vertical error bars, respectively.

LIST OF TABLES

I	Best EERs achieved by frontal face authentication algorithms within M2VTS project.	10
---	--	----

LIST OF FIGURES

1	Dilated and eroded images with a scaled hemisphere for scales 1–9.	10
2	Grid matching procedure in MDLA: (a) Model grid for person <i>BP</i> . (b) Best grid for test person <i>BP</i> after elastic graph matching with the model grid. (c) Best grid for test person <i>BS</i> after elastic graph matching with the model grid for person <i>BP</i> . (d) Model grid for person <i>BS</i> . (e) Best grid for test person <i>BP</i> after elastic graph matching with the model grid for <i>BS</i> . (f) Best grid for test person <i>BS</i> after elastic graph matching with the model grid.	11
3	Experimental Protocol.	11
4	Receiver Operating Characteristics of MDLA with and without most discriminating features as well as when discriminatory power coefficients are derived at each grid node. The 95% confidence interval of FAR and FRR is indicated with horizontal and vertical error bars, respectively.	12